Memory-critical dynamical buildup of phonon-dressed Majorana fermions

Oliver Kaestle [1,*] Yue Sun,[2,3] Ying Hu,[2,3] and Alexander Carmele [1]

[1] *Institut für Theoretische Physik, Nichtlineare Optik und Quantenelektronik, Technische Universität Berlin, Hardenbergstrasse 36, 10623 Berlin, Germany*

[2] *State Key Laboratory of Quantum Optics and Quantum Optics Devices, Institute of Laser Spectroscopy, Shanxi University, Taiyuan, Shanxi 030006, China*

[3] *Collaborative Innovation Center of Extreme Optics, Shanxi University, Taiyuan, Shanxi 030006, China*

(Received 2 July 2020; revised 24 November 2020; accepted 24 November 2020; published 11 December 2020)

We investigate the dynamical interplay between the topological state of matter and a non-Markovian dissipation, which gives rise to a crucial timescale into the system dynamics due to its quantum memory. We specifically study a one-dimensional polaronic topological superconductor with phonon-dressed p-wave pairing, when a fast temperature increase in surrounding phonons induces an open-system dynamics. We show that when the memory depth increases, the Majorana edge dynamics transits from relaxing monotonically to a plateau of substantial value into a collapse-and-buildup behavior, even when the polaron Hamiltonian is close to the topological phase boundary. Above a critical memory depth, the system can approach a new dressed state of the topological superconductor in dynamical equilibrium with phonons, with nearly full buildup of the Majorana correlation.

DOI: 10.1103/PhysRevB.102.245115

I. INTRODUCTION

Exploring topological properties out of equilibrium is central in the effort to realize, probe, and exploit topological states of matter in the laboratory [1–15]. A paradigmatic scenario is where the topological system is coupled to a Markovian bath, inducing open-dissipative dynamics that is described by a Lindblad-form master equation for the time-evolved reduced system density operator [16–28]. Yet solid-state realizations of topological matter, such as topological superconductors [29–40], are often based on semiconductor nanostructures, which are coupled to a structured phonon environment as a result of the deformation of host materials and its lattice vibrations. In this case, the Markovian approximation and thus the Lindblad formalism usually fail. Compared to Markovian scenarios, key differences arise from the presence of quantum memory effects in non-Markovian processes: The information is lost from the system to the environment but flows back at a *later time* [41,42]. This generates a timescale into the system dynamics that is strictly absent in a Markovian context and raises the challenge as to what the *unique* dynamical consequences of this interplay between the topological state of matter and non-Markovian dissipation are.

Here, we demonstrate that the quantum memory from a non-Markovian parity-preserving interaction of a topological p-wave superconductor with surrounding phonons can give rise to intriguing edge mode relaxation dynamics without a Markovian counterpart. Our study is based on the polaron master equation, describing open-dissipative dynamics of a *polaronic* topological superconductor with *phonon-renormalized* Hamiltonian parameters (see Fig. 1). In contrast to Markovian decoherence that typically destroys topological features for long times, we show that a finite quantum memory allows for substantial preservation of topological properties far from equilibrium, even when the polaron Hamiltonian is close to the topological phase boundary [see Fig. 2(b)]. Depending on the memory depth (i.e., the characteristic timescale of the quantum memory), the Majorana edge dynamics can monotonically relax to a plateau, or it undergoes a collapse-and-buildup relaxation [see Fig. 2(c)]. Remarkably, when the memory depth increases above a critical value, the edge correlation can nearly fully build up, corresponding to a *new polaronic state* of the topological superconductor in dynamical equilibrium with phonons.

II. POLARONIC KITAEV CHAIN

Concretely, we consider the paradigmatic Kitaev p-wave superconductor [43], with super-Ohmic coupling to a three-dimensional (3D) structured phonon reservoir. The total Hamiltonian is denoted by $H_0 = H_\mathrm{k} + H_\mathrm{b}$ ($\hbar \equiv 1$). The Kitaev Hamiltonian $H_\mathrm{k} = \sum_{l=1}^{N-1}[(-Jc_l^\dagger c_{l+1} + \Delta c_l c_{l+1}) + \mathrm{H.c.}] - \mu \sum_{l=1}^{N} c_l^\dagger c_l$ describes spinless fermions c_l and $c_l^\dagger$ on a chain of N sites l, with a nearest-neighbor tunneling amplitude $J \in \mathbb{R}$, pairing amplitude $\Delta \in \mathbb{R}$, and chemical potential μ. When $|\mu| < 2J$ and $\Delta \neq 0$, it is in the topological regime featuring unpaired Majorana edge modes $\gamma_{L/R} = \sum_{j=1} f_{L/R,j} b_j$ [here, we use the Majorana operators $b_{2j-1} = c_j + c_j^\dagger$ and $b_{2j} = -i(c_j - c_j^\dagger)$], with $f_{L/R,j}$ being exponentially localized near the left (L) and right (R) edges. The Majorana modes exhibit a nonlocal correlation $\theta = -i\langle\gamma_L\gamma_R\rangle = \pm 1$ that corresponds to the fermionic parity of the (degenerate) ground

*o.kaestle@tu-berlin.de

 ©2020 American Physical Society

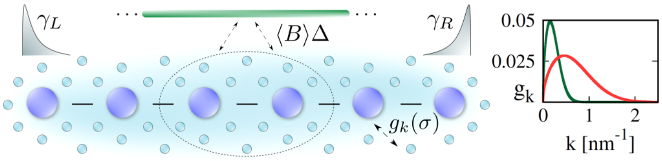

FIG. 1. Left: A polaronic Kitaev chain, with phonon-dressed spinless fermions, exhibits a renormalized p-wave pairing $\langle B\rangle\Delta$ at temperature T [see Eq. (1)]. In the topological ground state, two unpaired Majorana edge modes, γ_L and γ_R, emerge. The coupling g_k to the structured phonon bath features mode dependence with spectral width σ. Right: Gaussian profile of g_k in momentum space for $\sigma = 0.2$ (green) and $\sigma = 0.6$ (red).

states. The entire chain is coupled to a 3D structured phonon reservoir with a parity-preserving interaction, described by $H_\mathrm{b} = \int d^3k\ [\omega_{\boldsymbol k} r_{\boldsymbol k}^\dagger r_{\boldsymbol k} + \sum_{l=1}^N g_{\boldsymbol k} c_l^\dagger c_l (r_{\boldsymbol k}^\dagger + r_{\boldsymbol k})]$ [44–52]. Here, the operator $r_{\boldsymbol k}^{(\dagger)}$ annihilates (creates) phonons with momentum $\boldsymbol k$ and frequencies $\omega_k = c_s k$, where c_s is the sound velocity of the environment. This coupling is commonly applied for the description of polaron formation [53–58] and in solid-state setups can represent the coupling of semiconductor nanostructures to longitudinal acoustic phonons, which typically feature a long wavelength. We choose a generic super-Ohmic fermion-phonon coupling $g_{\boldsymbol k}$ which features frequency dependence modeled as a Gaussian function, $g_k = f_\mathrm{ph}\sqrt{k/\sigma^2}\exp(-k^2/\sigma^2)$, with σ being the width and f_{ph} being a dimensionless amplitude. We consider the topological superconductor and bath to be initially in equilibrium at low temperatures, before a fast increase in the bath temperature induces an open-system dynamics.

III. POLARON MASTER EQUATION

At the heart of our following solution lies the polaron representation of the coupled system (see Fig. 1). We derive a master equation in second-order perturbation theory of the *dressed-state* system-reservoir Hamiltonian [59]. In this dressed-state picture, the coherent process (i.e., higher-order contributions) from the fermion-phonon interaction is retained through *phonon-renormalized* Hamiltonian parameters [53–58,60–64]. In this way, we efficiently account for the non-Markovian character of the dynamics in the long-time limit not accessible and not captured in the typical second-order Born approximation of the bare-interaction Hamiltonian H_b [44–47].

Defining collective bosonic operators $R^\dagger = \int d^3k\ (g_k/\omega_k) r_{\boldsymbol k}^\dagger$, we apply a polaron transformation $U_\mathrm{p} = \exp[\sum_{l=1}^N c_l^\dagger c_l (R^\dagger - R)]$ resulting in $c_l^\dagger \to e^{-(R-R^\dagger)} c_l^\dagger$, which describes phonon dressing of fermions. The transformed total Hamiltonian $H_\mathrm{p} \equiv U_\mathrm{p} H_0 U_\mathrm{p}^{-1}$ is derived as

$$H_\mathrm{p} = \sum_{l=1}^{N-1}[-Jc_l^\dagger c_{l+1} + \Delta e^{-2(R-R^\dagger)} c_{l+1}^\dagger c_l^\dagger + \mathrm{H.c.}] - \mu \sum_{l=1}^N c_l^\dagger c_l + \int \mathrm{d}^3k\ \omega_k r_{\boldsymbol k}^\dagger r_{\boldsymbol k}. \tag{1}$$

Thus, the considered fermion-phonon interaction results in a polaronic Kitaev chain featuring phonon-dressed p-wave pairing, with phonon-induced quantum fluctuations. In deriving Eq. (1), we have ignored an arising energy renormalization term $H_\mathrm{shift} = \int d^3k\ (g_k^2/\omega_k)(\sum_{l=1}^N c_l^\dagger c_l)^2$, known as the polaron shift. In the context of non-Markovian dynamics, it is standard practice to neglect this term if the initial condition is equilibrium [60,65], which is the case in the present work, where the initial state is assumed to be the ground state of an ideal Kitaev chain. However, to ensure validity of our results even in the presence of this energy renormalization, in Appendix A we provide additional numerically exact calculations in the presence of the polaron energy shift, demonstrating that its inclusion does not affect the essential physics presented below. Before tracing out the phononic degrees of freedom, we rewrite Eq. (1) as $H_\mathrm{p} = H_\mathrm{p,s} + H_\mathrm{p,I} + H_\mathrm{p,b}$, with $H_\mathrm{p,b} = \int d^3k\ \omega_k r_{\boldsymbol k}^\dagger r_{\boldsymbol k}$ for the reservoir. To recover the bare Kitaev Hamiltonian dynamics for the limiting case $g_k \to 0$, we introduce a Franck-Condon renormalization of $H_\mathrm{p,I}$ satisfying $\mathrm{Tr}_B\{[H_\mathrm{p,I}, \rho(t)]\} = 0$, with $\rho(t)$ denoting the total density operator. The renormalized system Hamiltonian $H_\mathrm{p,s}$ is given by

$$H_\mathrm{p,s} = \sum_{l=1}^{N-1}[-Jc_l^\dagger c_{l+1} + \Delta\langle B\rangle c_{l+1}^\dagger c_l^\dagger + \mathrm{H.c.}] - \mu\sum_{l=1}^N c_l^\dagger c_l, \tag{2}$$

where the pairing renormalization factor $\langle B\rangle$ is given explicitly below. The system-reservoir interaction in the polaron picture reads $H_\mathrm{p,I} = \Delta\sum_{l=1}^{N-1}[(e^{-2(R-R^\dagger)} - \langle B\rangle)c_{l+1}^\dagger c_l^\dagger + \mathrm{H.c.}]$.

We will focus on the limit $\langle B\rangle \ll 1$, which allows us to treat $H_\mathrm{p,I}$ perturbatively in second-order Born theory, as dynamical decoupling effects cannot occur [57,60]. In Appendix B, we provide a detailed derivation of the polaron master equation for the reduced system density matrix $\rho_S(t)$ of the polaron chain, obtaining

$$\begin{aligned}\partial_t \rho_S(t) = &-i[H_\mathrm{p,s}, \rho_S(t)] - \langle B\rangle^2 \int_0^t d\tau \\ &\times (\{\cosh[\phi(\tau)] - 1\}\,[X_a, X_a(-\tau)\rho_S(t)] \\ &- \sinh[\phi(\tau)][X_b, X_b(-\tau)\rho_S(t)] + \mathrm{H.c.}).\end{aligned} \tag{3}$$

Here, $X_a = -\Delta\sum_{l=1}^{N-1}(c_l^\dagger c_{l+1}^\dagger + c_{l+1}c_l)$ and $X_b = \Delta\sum_{l=1}^{N-1}(c_l^\dagger c_{l+1}^\dagger - c_{l+1}c_l)$ denote collective system operators, whose dynamics obeys a *time-reversed* unitary evolution governed by the renormalized Hamiltonian $H_\mathrm{p,s}$, $X_{a,b}(-\tau) \equiv e^{-iH_\mathrm{p,s}\tau} X_{a,b} e^{iH_\mathrm{p,s}\tau}$. $\phi(\tau)$ represents the phonon correlation function,

$$\phi(\tau) = \int d^3k\ |2g_k(\sigma)/\omega_k|^2 \times \left[\coth\left(\frac{\hbar\omega_k}{2k_BT}\right)\cos(\omega_k\tau) - i\sin(\omega_k\tau)\right], \tag{4}$$

with k_B being the Boltzmann constant. The renormalization factor $\langle B\rangle$ in Eq. (2) is determined by the initial phonon correlation, $\langle B\rangle = \exp[-\phi(0)/2]$, with temperature dependence [66].

Equation (3) provides the key equation for our study. It features a *phonon-renormalized* Hamiltonian $H_\mathrm{p,s}$ and a memory kernel involving both reservoir and system correlators $\phi(\tau)$

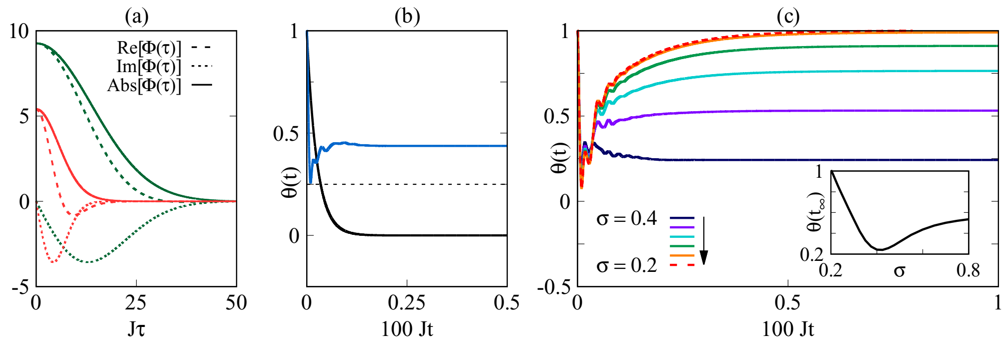

FIG. 2. Non-Markovian dynamics of the polaronic topological superconductor. (a) Phonon correlation function $\phi(\tau)$ for bandwidth $\sigma = 0.2$ (green) and $\sigma = 0.6$ (red) of the fermion-phonon coupling g_k. (b) Comparisons of Majorana correlation $\theta(t)$ calculated using the time-independent Lindblad-type master equation for dephasing (solid black line) and Eq. (3) with fully accounting for memory (solid blue line). The dashed black line shows asymptotic $\theta(t)$ in a coherent quench scenario $\Delta \rightarrow \Delta\langle B\rangle$. (c) Non-Markovian dynamics of $\theta(t)$ for various bandwidths σ of phonon coupling. The corresponding steady-state value $\theta(t_\infty)$ is shown as a function of σ in the inset. In all plots, we choose $N = 4$, $J = \Delta = 0.01$, $\mu = 0$; the amplitude of g_k is taken to be $f_{\rm ph} = 0.1$, and phonon modes within $k \in [0.0, 4.0]\,\mathrm{nm}^{-1}$ are considered.

and $X_{a,b}(-\tau)$. Crucially, the correlation of a super-Ohmic phonon bath has a finite lifetime [see Fig. 2(a)], $\phi(\tau) \approx 0$ for $\tau > \tau_M$. Therefore, at times $t > \tau_M$, only those $X_{a,b}(-\tau)$ within the past times $\tau \leqslant \tau_M$ contribute to the integral in Eq. (3). That is, the memory has a finite depth $\sim\tau_M$, so that for $t > \tau_M$ the integral becomes essentially time independent. The memory effect is substantial when $X_{a,b}(-\tau)$ evolves on a timescale, typically determined by E_Δ^{-1}, where E_Δ is the bulk gap of $H_{\rm p,s}$, comparable to τ_M. For given temperature and sound velocity c_s, $\phi(\tau)$ and τ_M critically depend on the bandwidth σ of fermion-phonon coupling g_k [see Fig. 2(a)]: A larger σ yields a smaller τ_M and at the same time leads to a smaller $\phi(0)$ and thus a larger $\langle B\rangle$.

Below we investigate the Majorana mode correlation $\theta(t) = -i\mathrm{Tr}[\rho_S(t)\gamma_L\gamma_j] = -\sum_{i,l=1}^{2N} f_{L,i} f_{R,l} \Gamma_{il}(t)$ [24]. Here, $\Gamma_{il}(t) = \frac{i}{2}\mathrm{Tr}\{\rho(t)[b_i, b_l]\}$, and $f_{L/R,i}$ are the Majorana wave functions of the *initial* Kitaev Hamiltonian in the Majorana basis. For concreteness, we assume the system is initially in the even-parity ground state of a perfect Kitaev chain with $\Delta = J$ and $\mu = 0$, where $f_{L,i} = \delta_{i,1}$ and $f_{R,l} = \delta_{l,2N}$, such that $\theta(t)$ reduces to $\theta(t) = -\Gamma_{1,2N}(t)$. Then, a fast increase of temperature to $T = 4$ K results in $\Delta \rightarrow \Delta\langle B\rangle$ of the dressed Hamiltonian, thus inducing the dynamics of the polaron chain for times $t > 0$. Due to the numerically very expensive size of the density matrix and its memory kernel, computations are performed for $N = 4$ sites.

IV. MEMORY: LOSS VERSUS REPHASING OF TOPOLOGICAL PROPERTIES

In Fig. 2(b), the solid blue line shows the non-Markovian dynamics of $\theta(t)$ for $\sigma = 0.6$ (corresponding to $\langle B\rangle = 0.07$), which decays to a substantial value. Compared to the Markovian decoherence which eventually destroys Majorana modes (solid black line), the long-lived and substantial Majorana correlation seen in the non-Markovian dynamics is quite remarkable, particularly given that $H_{\rm p,s}$ is near the topological phase boundary due to a significantly suppressed renormalized pairing $\Delta\langle B\rangle \ll \Delta$. Indeed, without the dissipation in Eq. (3), the dynamics formally reduces to that of a coherent quench in the pairing from Δ to $\Delta\langle B\rangle$. There, the Majorana correlation would approach an asymptotic value determined by the overlap of the edge mode wave functions for the pre- and postquench topological Hamiltonians [24], which is small if the postquench Hamiltonian is near the phase boundary (dashed black line). This differs significantly from the non-Markovian behavior in Fig. 2(b) and underscores the essential role of the memory effect.

A unique feature of the memory effect is that it, because of the dependence on both $\phi(\tau)$ and the reversed dynamics of system correlations $X_{a,b}(-\tau)$, *simultaneously* introduces decoherence and backflow of coherence. The dynamical consequence of these two competing processes can be intuitively understood as follows: The dressed Kitaev wire initially in its ground state is perturbed by a temperature increase to T, resulting in a renormalization of the polaron chain towards the phase boundary via $\phi(0) = \int d^3k\, |2g_k(\sigma)/\omega_k|^2 \coth[\hbar\omega_k/(2k_BT)]$, which generates significant bulk excitations and populates the Majorana edge mode, changing the parity of Majorana states. Combined with phonon-assisted dephasing, this leads to strong decoherence in the polaronic Kitaev wire. On the other hand, the reversed dynamics of $X_{a,b}(-\tau)$ acts to reinstate the coherence of the p-wave pairing that is the key ingredient for a topological wire. Such a rephasing effect is marginal, at times smaller than τ_M, so an irreversible loss of parity information dominates the short-time dynamics. Once $\phi(\tau)$ decays to zero at large times $\tau > \tau_M$, the memory reaches its full depth, and the rephasing of topological properties grows due to $X_{a,b}(-\tau)$, giving a considerable Majorana correlation in Fig. 2(b). While the calculated system is small, we remark that this asymptotic nonlocal correlation is not due to phonon-mediated long-range interaction and is of topological origin, as we can show that the correlations decay with relative spacing, whereas the edge-edge correlation is significant (see Appendix C).

V. CRITICAL MEMORY DEPTH

We find the edge dynamics can exhibit distinct relaxation behavior depending crucially on the memory depth, tunable through the bandwidth σ of fermion-phonon coupling. Figure 2(c) presents the non-Markovian dynamics of $\theta(t)$ for various σ. Compared to $\sigma = 0.6$ [blue line in Fig. 2(b)], an initial decrease of σ results in a steeper monotonic decay of $\theta(t)$ and a smaller asymptotic value [blue line in Fig. 2(c)]. However, when σ decreases further, the monotonic relaxation transits into a nonmonotonic one: While the short-time decoherence is accelerated, a buildup of edge correlation nonetheless occurs at some large times (purple line). Such a buildup becomes stronger with decreasing σ, approaching an asymptotic value larger than the $\sigma = 0.6$ case (turquoise and green lines). Strikingly, once σ surpasses a critical value, the asymptotic Majorana correlation approaches $\theta(t_\infty) \to 1$ (orange and dashed red lines). The inset in Fig. 2(c) summarizes the nonmonotonic variation of $\theta(t_\infty)$: When σ decreases from a large value, $\theta(t_\infty)$ first decreases to a minimum and then increases toward unity.

Insights into the above intriguing phenomena can be obtained from the fact that reducing σ leads to an increased lifetime of $\phi(\tau)$ and therefore increased memory, at the cost of a smaller $\langle B\rangle = \exp[-\phi(0)/2]$ [see Fig. 2(a)]. The former enhances the timescale of the time-reversed evolution of $X_{a,b}(-\tau)$ and hence the rephasing of pairing, whereas the latter further suppresses the bulk gap E_Δ of $H_{\mathrm{p,s}}$ as well as weakening the memory strength. When σ is initially decreased from 0.6, the latter effect dominates, aggravating the decay. With further reduction of σ, however, the former rephasing effect grows, allowing phonons and fermions to synchronize and hence inducing backflow of parity information. Consequently, a new dressed state manages to emerge, with buildup of Majorana correlation starting to dominate over decoherence. In general, we estimate the recovery of correlation can begin at times $t > \tau_M$ if $E_\Delta \tau_M \gtrsim 1$ is satisfied. Importantly, the existence of a critical σ indicates a critical memory depth, above which the system asymptotically approaches a new polaronic steady state in dynamical equilibrium with phonons at $T = 4\,\mathrm{K}$, which can remarkably exhibit $\theta \approx 1$. The critical value of σ in our case is between 0.21 and 0.20, corresponding to $\langle B\rangle = 0.01$, but it is model specific. We note that the fermion-phonon coupling bandwidth can be controlled, such as in solid-state setups with nanotechnological design, e.g., alloys, impurities, and confinement potentials [67–70].

VI. CONCLUDING DISCUSSION

The central results of our work shown in Fig. 2 are found to be robust for initially nonideal Kitaev chains (see Appendix D) and other forms of super-Ohmic coupling. In the presence of perturbation caused by weak attractive p-wave interactions, we find a speedup of the revival of Majorana correlation. Specifically, in Fig. 3, we calculate the non-Markovian evolution of $\theta(t)$ by including $H_{\mathrm{int}} = U\sum_{l=1}^{N-1}(c_l^\dagger c_l - 1/2)(c_{l+1}^\dagger c_{l+1} - 1/2)$ with interaction strength $|U| \ll 1$ in $H_{\mathrm{p,s}}$ of Eq. (3) for $\sigma = 0.6$. The interaction is treated exactly in our numerical solution, which is mandatory since resorting to approximate descriptions such as a mean-field approach would inevitably destroy entanglement in the system over time. Compared to the $U = 0$ case (blue line), we see that adding a weak attractive interaction $U < 0$ not only shortens the time needed to reach the steady state, but it can further enhance, depending on $|U|$, the asymptotic

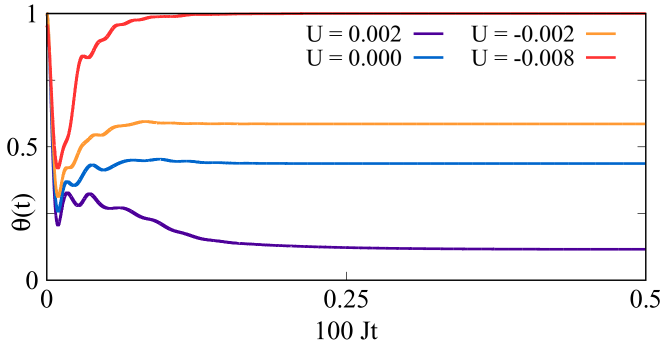

FIG. 3. Non-Markovian Majorana dynamics for the renormalized Hamiltonian $H_{\mathrm{p,s}}$ in the presence of weak p-wave interaction, $H_{\mathrm{int}} = U\sum_{l=1}^{N-1}(c_l^\dagger c_l - 1/2)(c_{l+1}^\dagger c_{l+1} - 1/2)$. Calculations are performed at $N = 4$, $J = \Delta = 0.01$, $\mu = 0$, and $\sigma = 0.6$.

Majorana correlation for subcritical memory depth (orange and red lines). An intuitive understanding can be obtained by noting that the attractive interaction is energetically favorable for coherent formation of superconductive pairing, which provides a mechanism to counteract the aforementioned phonon-induced dephasing. This is consistent with the observation that for $U > 0$, $\theta(t)$ significantly declines from the $U = 0$ case at long times (purple line), as repulsive interactions energetically suppress pairing.

Summarizing, we have demonstrated memory-critical edge dynamics in a topological superconductor with non-Markovian interaction with phonons, resulting in a revival of topological properties. We show this intriguing phenomenon uniquely arises from the interplay between the phonon-renormalized topological Hamiltonian and the quantum memory effect that simultaneously induces dephasing and information backflow. Our analysis is based on the Kitaev chain, but we expect the essential physics to occur for a wide class of topological materials coupled to a super-Ohmic reservoir. Currently, there are significant efforts in the condensed-matter context aimed at realizing Majorana fermions based on the hybrid superconductor and semiconductor nanowires. The phonon-fermion coupling described here is relevant for InAs nanowires [29–34], where the acoustic phonons of InAs are in the range of typical nanowire length realization up to 100 nm and have super-Ohmic coupling as investigated in our study. In a broader context, we anticipate the fundamental non-Markovian feature of reservoir-induced recovery of topological properties may also be seen in cold-atom setups where phonons stem from the excitations of the superfluid reservoir coupled to ultracold quantum gases [71–73] or in setups where a coupling to bosons is intentionally induced as long as such coupling is structured and induces non-Markovian system-reservoir correlations. We finally note our work is different from some recent work on topological systems which also considered non-Markovian system-bath interactions. In Refs. [74–76] an impurity or a qubit is employed as a non-Markovian quantum probe of a topological reservoir, and Ref. [77] shows that a topological phenomenon induced by a Markovian dissipation can persist in non-Markovian regimes. In contrast, our study demonstrated that tailoring the coupling to a super-Ohmic reservoir may suppress the loss of, and even fully restore, topological properties, which opens an appealing prospect as to the explorations and control of memory-dependent topological phenomena.

ACKNOWLEDGMENTS

O.K. and A.C. acknowledge support from the Deutsche Forschungsgemeinschaft (DFG) through SFB 910 project B1 (Project No. 163436311). Y.H. acknowledges the National Natural Science Foundation of China (Grant No. 11874038).

APPENDIX A: POLARON SHIFT

The polaron transformation of the open-system Hamiltonian yields an additional term,

$$H_{\text{shift}} = \int d^3k \, \frac{g_k^2}{\omega_k} \left(\sum_{l=1}^{N} c_l^\dagger c_l \right)^2, \tag{A1}$$

which is known as the polaron shift describing a polaron-induced energy renormalization. In the present study, we are justified to neglect this polaron shift under proper conditions: In the context of non-Markovian dynamics, it is standard practice to neglect this polaron shift if *the initial condition is equilibrium*, along the lines of Leggett (see, e.g., Refs. [60,65] and references therein). In our study, the initial state is assumed to be the ground state of a Kitaev chain, and therefore, the polaron shift is ignored according to the convention. We do not discuss a generic account of the polaron shift beyond the aforementioned condition, which remains, to date, an open question in the context of the non-Markovian community and is, of course, beyond the scope of our current work.

Nonetheless, to demonstrate that our qualitative results are invariant against this energy renormalization, we provide calculations in the presence of the polaron energy shift, which are treated numerically exactly. In Fig. 4, we show the resulting non-Markovian dynamics of Majorana correlation including H_{shift}. In addition, in the inset in Fig. 4, the steady-state correlations for various σ are compared for the cases including the polaron shift (solid line) and disregarding it (dashed line). As can be seen from Fig. 4, including the polaron shift does not change the qualitative behavior and memory-critical buildup of the Majorana correlation. The polaron shift term is proportional to the width σ of the coupling. However, this merely affects the number of nonzero phonon modes taken into account for the energy renormalization, resulting in a plateau of the steady-state correlation at intermediate σ and slightly decreased steady-state values at large σ (see the inset plot in Fig. 4). This is not to be confused with the large impact of σ on the correlation described in the main text, which originates from the strong dependence of the lifetime of the phonon correlation $\phi(\tau)$ on σ.

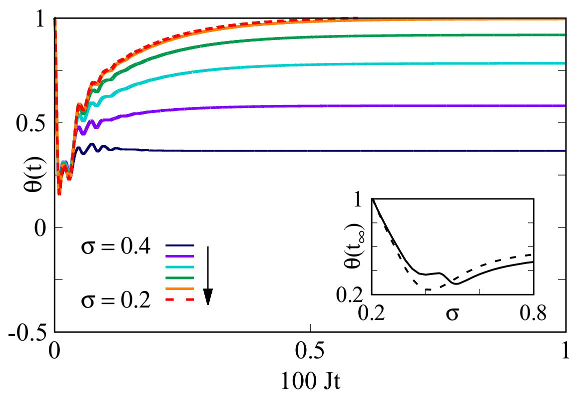

FIG. 4. Non-Markovian dynamics of the polaronic Majorana correlation $\theta(t)$ for various bandwidths σ of the phonon coupling. Here, calculations include the polaron shift term H_{shift}. The corresponding steady state value $\theta(t_\infty)$ is shown as a function of σ in the inset, comparing the cases including the polaron shift (solid line) and disregarding it (dashed line). We have used $N = 4$, $J = \Delta = 0.01$, $\mu = 0$, $f_{\text{ph}} = 0.1$, and phonon modes within $k \in [0.0, 4.0]\,\text{nm}^{-1}$ are considered.

APPENDIX B: POLARON MASTER EQUATION

For the description of the non-Markovian open-system dynamics, the polaron master equation is employed. It is derived in second-order perturbation theory of the polaron-transformed, dressed-state system-reservoir Hamiltonian. Phonon contributions are traced out in the process, while higher-order contributions of the fermion-phonon interactions by the phonon-renormalized Hamiltonian are still accounted for [53–58,60,61]. For the derivation of the master equation in the polaron picture, the perturbative expansion is performed with respect to the *phonon-renormalized* superconducting gap $\Delta\langle B\rangle$, with $\langle B\rangle \ll 1$. The parameter $\Delta\langle B\rangle$ is defined in the polaronic frame and addresses the strong fermion-phonon correlations in question.

The von Neumann equation $\partial_t \rho(t) = i/\hbar[H, \rho(t)]$ is formally solved by integration and reinserted into itself. First, it is assumed that the environment is large compared to the system and initially in a thermal equilibrium state, known as the bath assumption. As a consequence, the reservoir is assumed to be a Gaussian bath with a defined temperature. Under these conditions, the Born approximation then is applied, assuming a weak system-bath interaction. As a consequence of weak coupling between the system and reservoir, the latter is not perturbed by excitation transfer from the system. Hence, it remains in its initial equilibrium state for all times, $\rho_B(t) \approx \rho_B(0)$, and the density matrix factorizes under these assumptions [60]: $\rho(t-\tau) \approx \rho_S(t-\tau) \otimes \rho_B(0)$, with indices S and B denoting the system and reservoir parts of the density matrix $\rho(t)$, respectively. Here, τ denotes past times that are taken into account for the calculation of the current state within the scope of the second-order perturbative treatment. In addition, the first Markovian approximation is applied, during which the history of the system part of the state is disregarded: $\rho_S(t-\tau) \approx \rho_S(t)$. It is assumed that the current state is mainly determined by the previous system state alone, which is again valid if the influence from the reservoir is weak. However, the interaction between the system and the reservoir itself maintains a history, as the influence of the phonons is taken into account on their own timescale. As a result, the interaction has a memory. Tracing out the phonon degrees of freedom results in the non-Markovian Redfield master equation for the reduced system density matrix ρ_S [60],

$$\partial_t \rho_S(t) = -i\mathrm{Tr}_B\{[H_{\mathrm{p,s}} + H_{\mathrm{p,b}} + H_{\mathrm{p,I}}, \rho_S(t) \otimes \rho_B]\} - \int_0^t d\tau \mathrm{Tr}_B\{[H_{\mathrm{p,I}}, [H_{\mathrm{p,I}}(-\tau), \rho_S(t) \otimes \rho_B]]\}. \quad \text{(B1)}$$

We define collective system and reservoir operators

$$X_a(t) = -\Delta \sum_{l=1}^{N-1} (c_l^\dagger c_{l+1}^\dagger + c_{l+1} c_l), \quad \text{(B2)}$$

$$X_b(t) = \Delta \sum_{l=1}^{N-1} (c_l^\dagger c_{l+1}^\dagger - c_{l+1} c_l), \quad \text{(B3)}$$

and

$$B_a(t) = e^{2[R(t)-R^\dagger(t)]} + e^{-2[R(t)-R^\dagger(t)]}, \quad \text{(B4)}$$

$$B_b(t) = e^{2[R(t)-R^\dagger(t)]} - e^{-2[R(t)-R^\dagger(t)]}, \quad \text{(B5)}$$

with $R^\dagger = \int d^3k\ (g_k/\omega_k) r_{\mathbf{k}}^\dagger$. The Franck-Condon renormalized, polaron-transformed interaction Hamiltonian then takes the form

$$H_{\mathrm{p,I}}(t) = \tfrac{1}{2} X_a(t)[B_a(t) - \langle B_a \rangle] + \tfrac{1}{2} X_b(t) B_b(t). \quad \text{(B6)}$$

As a next step, the integrand of Eq. (B1) is calculated. Assuming the phonon number n_k is a Bose distribution, resulting in $(2n_k + 1) = \coth[\hbar\omega_k/(2k_B T)]$, and making use of the Baker-Campbell-Hausdorff formula, the time-reversed bath correlations of the form $\langle B_{a,b} B_{a,b}(-\tau)\rangle$, $\langle B_{a,b}(-\tau) B_{a,b}\rangle$ can be evaluated. We define the phonon correlation function

$$\phi(\tau) = \int d^3k\ |2g_k(\sigma)/\omega_k|^2 \times \left[\coth\left(\frac{\hbar\omega_k}{2k_B T}\right)\cos(\omega_k \tau) - i \sin(\omega_k \tau)\right] \quad \text{(B7)}$$

and arrive at the final form of the bath correlations,

$$\begin{aligned} \langle B_a B_a(-\tau)\rangle &= 4\exp[-\phi(0)]\cosh[\phi(\tau)], \\ \langle B_b B_b(-\tau)\rangle &= -4\exp[-\phi(0)]\sinh[\phi(\tau)], \end{aligned} \quad \text{(B8)}$$

with $\langle B_{a,b} B_{a,b}(-\tau)\rangle = \langle B_{a,b}(-\tau) B_{a,b}\rangle^*$. Inserting these expressions into Eq. (B1), we arrive at the polaron master equation

$$\begin{aligned} \partial_t \rho_S(t) = &-i[H_{\mathrm{p,s}}, \rho_S(t)] - e^{-\phi(0)} \int_0^t d\tau \\ &\times (\{\cosh[\phi(\tau)] - 1\}[X_a, X_a(-\tau)\rho_S(t)] \\ &- \sinh[\phi(\tau)][X_b, X_b(-\tau)\rho_S(t)] + \mathrm{H.c.}), \end{aligned} \quad \text{(B9)}$$

which, due to the limits of the applied approximations, is valid for the case of weak system-reservoir interactions [41,42]. The initial separability of the system and reservoir is justified by the assumed initial state featuring a Majorana correlation. Afterwards, separability is ensured by the bath assumption and Born approximation as long as we remain in the weak-coupling regime $\langle B\rangle \ll 1$, where the polaron master equation holds.

For the calculation of the full system-reservoir memory kernel, the time evolution of the system correlators $X_{a,b}(-\tau)$ is determined by the static part of the polaron Hamiltonian, $X_{a,b}(-\tau) = e^{-iH_{\mathrm{p,s}}\tau} X_{a,b} e^{iH_{\mathrm{p,s}}\tau}$. We get, for a specific matrix element,

$$\begin{aligned} \langle m| X_{a,b}(-\tau) |n\rangle &= \sum_{\{s\}} \langle m| U(\tau,0) X_{a,b} |s\rangle \langle s| U^\dagger(\tau,0) |n\rangle \\ &= \sum_{\{s\}} \langle s| U^\dagger(\tau,0) \underbrace{|n\rangle\langle m|}_{=:\rho_c(0)} U(\tau,0) X_{a,b} |s\rangle \\ &= \mathrm{Tr}\{\rho_c(-\tau) X_{a,b}\}, \end{aligned} \quad \text{(B10)}$$

with $|n\rangle = |n_1, n_2, \ldots, n_N\rangle$ and site occupations $n_l = \{0, 1\}$. Here, we introduced the conditional density matrix $\rho_c(-\tau)$, whose time evolution dynamics must be determined for all possible initial conditions $\rho_c(0) = |n\rangle\langle m|$, i.e., with $\langle n| \rho_c(0) |m\rangle = 1$ and all other entries being zero. The dynamics of $\rho_c(t)$ is provided by $\partial_t \rho_c(t) = -i[H_{\mathrm{p,s}}, \rho_c(t)]$. For the numerical solution of the integro-differential polaron master equation, we employ two nested fourth-order Runge-Kutta algorithms: (i) The first time integration is required to evaluate the integral over all past times, which consists of the system correlators $X_{a,b}(-\tau) = e^{-iH_{\mathrm{p,s}}\tau} X_{a,b} e^{iH_{\mathrm{p,s}}\tau}$ and the time-dependent phonon correlation function $\phi(\tau)$. (ii) In a second time integration, the reduced system time evolution dynamics are calculated using the previously determined integral up to the current time step.

To investigate the robustness of Majorana edge states in the Kitaev chain, we calculate the Majorana edge-edge correlation. In the case of an ideal Kitaev chain it is given by $-i\langle \gamma_L \gamma_R\rangle(t) = \mathrm{Tr}\{\rho(t)(c_1 + c_1^\dagger)(c_N^\dagger - c_N)\}$. Assuming even parity conditions, i.e., $\sum_{l=1}^N n_l = 2\nu$, $\nu \in \mathbb{N}_0$ in the Jordan-Wigner phase factor, this yields

$$\begin{aligned} \langle\theta\rangle(t) = \sum_{\{n\}} [&\langle 1, n_2, \ldots, n_{N-1}, 0| \rho(t) |0, n_2, \ldots, n_{N-1}, 1\rangle \\ &+ \langle 0, n_2, \ldots, n_{N-1}, 1| \rho(t) |1, n_2, \ldots, n_{N-1}, 0\rangle \\ &+ \langle 0, n_2, \ldots, n_{N-1}, 0| \rho(t) |1, n_2, \ldots, n_{N-1}, 1\rangle \\ &+ \langle 1, n_2, \ldots, n_{N-1}, 1| \rho(t) |0, n_2, \ldots, n_{N-1}, 0\rangle]. \end{aligned} \quad \text{(B11)}$$

APPENDIX C: TOPOLOGICAL CORRELATION

Due to the numerically expensive calculation of the density matrix and the finite memory kernel of the polaron master equation, the considered chain size is chosen at $N = 4$ sites. Here, we demonstrate that the observed Majorana correlation at long times is genuinely of topological origin, rather than caused by phonon-mediated long-range correlations. To this end, we calculate the asymptotic correlation $\lim_{t\to+\infty}\{-i\mathrm{Tr}[\rho_S(t) b_1 b_{2j}]\}$ between the Majorana operators b_1 and b_{2j} for lattice sites $j = 2, 3, 4$. Figure 5 shows the resulting correlation dynamics for widths $\sigma = \{0.6, 0.2\}$ of the fermion-phonon coupling element. We see that the correlation decays with the separation $d = j - 1$ and becomes vanishingly small for $d = 2$ but increases to attain a significant value at the right edge for $d = 3$. We see this phenomenon as a topological signature reflecting the nonlocal Majorana correlation because if the beyond-nearest-neighbor correlation for separation $d > 1$ originates from phonon-mediated effects, one would expect a monotonous decay with the two-site distance.

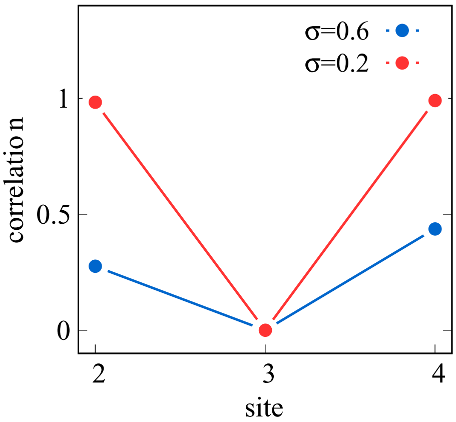

FIG. 5. The asymptotic correlation $-i\langle b_1 b_{2j}\rangle(t_\infty) = \lim_{t\to+\infty}\{-i\mathrm{Tr}[\rho_S(t)b_1b_{2j}]\}$ between Majorana operators b_1 and b_{2j} for lattice sites $j = 2, 3, 4$ in a Kitaev chain of length $N = 4$, respectively calculated at fermion-phonon coupling widths $\sigma = \{0.6, 0.2\}$. We take $J = \Delta = 0.01$, $\mu = 0$, $f_{\mathrm{ph}} = 0.1$.

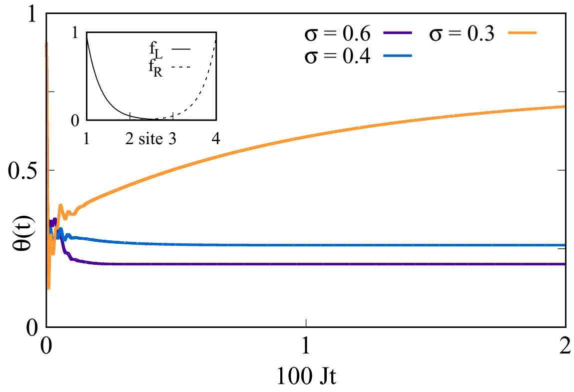

FIG. 6. Dynamics of the edge-edge correlation $-i\langle b_1 b_{2N}\rangle(t) = -i\mathrm{Tr}[\rho_S(t)b_1b_{2N}]$ for a nonideal Kitaev chain with $J = \Delta$, $\mu = 0.1\,\mathrm{J}$, and $N = 4$. Results for several coupling widths σ are shown.

APPENDIX D: NONIDEAL KITAEV CHAIN

In the main text we showed our results with an initially ideal Kitaev chain, where the overlap between the left and right Majorana modes is strictly zero even for a small system of four sites. If the initial Kitaev chain deviates away from the ideal case, the Majorana wave function $f_{L/R,i}$ extends into the bulk. But for very small deviations, it is still possible to find suitable parameter regimes to ensure a small overlap between Majorana modes for a four-site system. In Fig. 6, we present calculations for the edge-edge correlation $-i\mathrm{Tr}[\rho_S(t)b_1b_{2N}]$ for an initially nonideal initial Kitaev Hamiltonian with $J = \Delta$ and $\mu = 0.1J$, and still, we observe revival of the correlation when σ is tuned below a threshold value.

[1] N. Lindner, G. Refael, and V. Galitski, Nat. Phys. **7**, 490 (2011).
[2] T. Kitagawa, M. A. Broome, A. Fedrizzi, M. S. Rudner, E. Berg, I. Kassal, A. Aspuru-Guzik, E. Demler, and A. G. White, Nat. Commun. **3**, 882 (2012).
[3] G. Jotzu, M. Messer, R. Desbuquois, M. Lebrat, T. Uehlinger, D. Greif, and T. Esslinger, Nature (London) **515**, 237 (2014).
[4] D. Aasen, M. Hell, R. V. Mishmash, A. Higginbotham, J. Danon, M. Leijnse, T. S. Jespersen, J. A. Folk, C. M. Marcus, K. Flensberg, and J. Alicea, Phys. Rev. X **6**, 031016 (2016).
[5] Y. Hu, P. Zoller, and J. C. Budich, Phys. Rev. Lett. **117**, 126803 (2016).
[6] J. C. Budich, Y. Hu, and P. Zoller, Phys. Rev. Lett. **118**, 105302 (2017).
[7] N. Fläschner, D. Vogel, M. Tarnowski, B. S. Rem, D.-S. Lühmann, M. Heyl, J. C. Budich, L. Mathey, and K. Sengstock, Nat. Phys. **14**, 265 (2018).
[8] M. Tarnowski, F. N. Ünal, N. Fläschner, B. S. Rem, A. Eckardt, K. Sengstock, and C. Weitenberg, Nat. Commun. **10**, 1728 (2019).
[9] M. Heyl, Rep. Prog. Phys. **81**, 054001 (2018).
[10] W. Sun, C.-R. Yi, B.-Z. Wang, W.-W. Zhang, B. C. Sanders, X.-T. Xu, Z.-Y. Wang, J. Schmiedmayer, Y. Deng, X.-J. Liu, S. Chen, and J.-W. Pan, Phys. Rev. Lett. **121**, 250403 (2018).
[11] B. Song, C. He, S. Niu, L. Zhang, Z. Ren, X.-J. Liu, and G.-B. Jo, Nat. Phys. **15**, 911 (2019).
[12] L. Zhang, L. Zhang, S. Niu, and X.-J. Liu, Sci. Bull. **63**, 1385 (2018).
[13] Z. Shi, P. W. Brouwer, K. Flensberg, L. I. Glazman, and F. von Oppen, Phys. Rev. B **101**, 241414(R) (2020).
[14] J. W. McIver, B. Schulte, F.-U. Stein, T. Matsuyama, G. Jotzu, G. Meier, and A. Cavalleri, Nat. Phys. **16**, 38 (2020).
[15] A. Elben, J. Yu, G. Zhu, M. Hafezi, F. Pollmann, P. Zoller, and B. Vermersch, Sci. Adv. **6**, eaaz3666 (2020).
[16] M. S. Rudner and L. S. Levitov, Phys. Rev. Lett. **102**, 065703 (2009).
[17] S. Diehl, E. Rico, M. A. Baranov, and P. Zoller, Nat. Phys. **7**, 971 (2011).
[18] D. Rainis and D. Loss, Phys. Rev. B **85**, 174533 (2012).
[19] M. J. Schmidt, D. Rainis, and D. Loss, Phys. Rev. B **86**, 085414 (2012).
[20] M. Ippoliti, M. Rizzi, V. Giovannetti, and L. Mazza, Phys. Rev. A **93**, 062325 (2016).
[21] L. Mazza, M. Rizzi, M. D. Lukin, and J. I. Cirac, Phys. Rev. B **88**, 205142 (2013).
[22] C.-E. Bardyn, M. A. Baranov, C. V. Kraus, E. Rico, A. İmamoğlu, P. Zoller, and S. Diehl, New J. Phys. **15**, 085001 (2013).
[23] F. L. Pedrocchi and D. P. DiVincenzo, Phys. Rev. Lett. **115**, 120402 (2015).
[24] Y. Hu, Z. Cai, M. A. Baranov, and P. Zoller, Phys. Rev. B **92**, 165118 (2015).
[25] J. C. Budich, P. Zoller, and S. Diehl, Phys. Rev. A **91**, 042117 (2015).
[26] V. V. Albert, B. Bradlyn, M. Fraas, and L. Jiang, Phys. Rev. X **6**, 041031 (2016).
[27] Z. Gong, S. Higashikawa, and M. Ueda, Phys. Rev. Lett. **118**, 200401 (2017).
[28] S. Lieu, M. McGinley, and N. R. Cooper, Phys. Rev. Lett. **124**, 040401 (2020).

[29] Y. Oreg, G. Refael, and F. von Oppen, Phys. Rev. Lett. **105**, 177002 (2010).
[30] P. W. Brouwer, M. Duckheim, A. Romito, and F. von Oppen, Phys. Rev. Lett. **107**, 196804 (2011).
[31] V. Mourik, K. Zuo, S. M. Frolov, S. R. Plissard, E. P. A. M. Bakkers, and L. P. Kouwenhoven, Science **336**, 1003 (2012).
[32] L. P. Rokhinson, X. Liu, and J. K. Furdyna, Nat. Phys. **8**, 795 (2012).
[33] A. Das, Y. Ronen, Y. Most, Y. Oreg, M. Heiblum, and H. Shtrikman, Nat. Phys. **8**, 887 (2012).
[34] S. Nadj-Perge, I. K. Drozdov, J. Li, H. Chen, S. Jeon, J. Seo, A. H. MacDonald, B. A. Bernevig, and A. Yazdani, Science **346**, 602 (2014).
[35] H. O. H. Churchill, V. Fatemi, K. Grove-Rasmussen, M. T. Deng, P. Caroff, H. Q. Xu, and C. M. Marcus, Phys. Rev. B **87**, 241401(R) (2013).
[36] A. D. K. Finck, D. J. Van Harlingen, P. K. Mohseni, K. Jung, and X. Li, Phys. Rev. Lett. **110**, 126406 (2013).
[37] V. Fatemi, S. Wu, Y. Cao, L. Bretheau, Q. D. Gibson, K. Watanabe, T. Taniguchi, R. J. Cava, and P. Jarillo-Herrero, Science **362**, 926 (2018).
[38] D. Laroche, D. Bouman, D. J. van Woerkom, A. Proutski, C. Murthy, D. I. Pikulin, C. Nayak, R. J. J. van Gulik, J. Nygrd, P. Krogstrup, L. P. Kouwenhoven, and A. Geresdi, Nat. Commun. **10**, 245 (2019).
[39] A. Fornieri, A. M. Whiticar, F. Setiawan, E. Portolés, A. C. C. Drachmann, A. Keselman, S. Gronin, C. Thomas, T. Wang, R. Kallaher, G. C. Gardner, E. Berg, M. J. Manfra, A. Stern, C. M. Marcus, and F. Nichele, Nature (London) **569**, 89 (2019).
[40] H. Ren, F. Pientka, S. Hart, A. T. Pierce, M. Kosowsky, L. Lunczer, R. Schlereth, B. Scharf, E. M. Hankiewicz, L. W. Molenkamp, B. I. Halperin, and A. Yacoby, Nature (London) **569**, 93 (2019).
[41] H.-P. Breuer, E.-M. Laine, J. Piilo, and B. Vacchini, Rev. Mod. Phys. **88**, 021002 (2016).
[42] I. de Vega and D. Alonso, Rev. Mod. Phys. **89**, 015001 (2017).
[43] A. Y. Kitaev, Phys. Usp. **44**, 131 (2001).
[44] G. D. Mahan, *Many-Particle Physics* (Springer, Berlin, 2013).
[45] M. Kira and S. W. Koch, *Semiconductor Quantum Optics* (Cambridge University Press, Cambridge, 2011).
[46] V. May and O. Kühn, *Charge and Energy Transfer Dynamics in Molecular Systems* (Wiley, Hoboken, NJ, 2008).
[47] M. A. Stroscio and M. Dutta, *Phonons in Nanostructures* (Cambridge University Press, Cambridge, 2001).
[48] J. Förstner, C. Weber, J. Danckwerts, and A. Knorr, Phys. Rev. Lett. **91**, 127401 (2003).
[49] B. Krummheuer, V. M. Axt, and T. Kuhn, Phys. Rev. B **65**, 195313 (2002).
[50] A. Carmele, A. Knorr, and F. Milde, New J. Phys. **15**, 105024 (2013).
[51] N. Német, S. Parkins, A. Knorr, and A. Carmele, Phys. Rev. A **99**, 053809 (2019).
[52] D. Reiter, T. Kuhn, and V. M. Axt, Adv. Phys.: X **4**, 1655478 (2019).
[53] I. Wilson-Rae and A. Imamoğlu, Phys. Rev. B **65**, 235311 (2002).
[54] S. Weiler, A. Ulhaq, S. M. Ulrich, D. Richter, M. Jetter, P. Michler, C. Roy, and S. Hughes, Phys. Rev. B **86**, 241304(R) (2012).
[55] R. Manson, K. Roy-Choudhury, and S. Hughes, Phys. Rev. B **93**, 155423 (2016).
[56] C. K. Lee, J. Moix, and J. Cao, J. Chem. Phys. **136**, 204120 (2012).
[57] D. P. S. McCutcheon and A. Nazir, New J. Phys. **12**, 113042 (2010).
[58] H.-T. Chang, P.-P. Zhang, and Y.-C. Cheng, J. Chem. Phys. **139**, 224112 (2013).
[59] The polaron master equation is based on the first Markovian approximation, disregarding the history of the system part of the state, while the system-reservoir interaction maintains a history, as phonon influences are taken into account on their own timescale. The resulting master equation holds in the weak-coupling regime.
[60] H. P. Breuer and F. Petruccione, *The Theory of Open Quantum Systems* (Oxford University Press, Oxford, 2002).
[61] A. Carmele and S. Reitzenstein, Nanophotonics **8**, 655 (2019).
[62] M. Strauß, A. Carmele, J. Schleibner, M. Hohn, C. Schneider, S. Höfling, J. Wolters, and S. Reitzenstein, Phys. Rev. Lett. **122**, 107401 (2019).
[63] E. V. Denning, J. Iles-Smith, and J. Mork, Phys. Rev. B **100**, 214306 (2019).
[64] E. V. Denning, J. Iles-Smith, N. Gregersen, and J. Mork, Opt. Mater. Express **10**, 222 (2020).
[65] A. Caldeira and A. Leggett, Phys. A (Amsterdam, Neth.) **121**, 587 (1983).
[66] We solve the integro-differential equation numerically via two nested fourth-order Runge-Kutta algorithms: The first time integration is required to evaluate the integral over all past times τ. In a second time integration, the reduced system dynamics are calculated using the previously determined integral up to the current time step.
[67] W. Kim, J. Mater. Chem. C **3**, 10336 (2015).
[68] S. Xiong, K. Sääskilahti, Y. A. Kosevich, H. Han, D. Donadio, and S. Volz, Phys. Rev. Lett. **117**, 025503 (2016).
[69] A. A. Balandin, J. Nanosci. Nanotechnol. **5**, 1015 (2005).
[70] A. A. Balandin, E. P. Pokatilov, and D. L. Nika, J. Nanoelectron. Optoelectron. **2**, 140 (2007).
[71] L. Jiang, T. Kitagawa, J. Alicea, A. R. Akhmerov, D. Pekker, G. Refael, J. I. Cirac, E. Demler, M. D. Lukin, and P. Zoller, Phys. Rev. Lett. **106**, 220402 (2011).
[72] S. Nascimbène, J. Phys. B **46**, 134005 (2013).
[73] Y. Hu and M. A. Baranov, Phys. Rev. A **92**, 053615 (2015).
[74] F. Grusdt, N. Y. Yao, D. Abanin, M. Fleischhauer, and E. Demler, Nat. Commun. **7**, 11994 (2016).
[75] A. Camacho-Guardian, N. Goldman, P. Massignan, and G. M. Bruun, Phys. Rev. B **99**, 081105(R) (2019).
[76] G. L. Giorgi, S. Longhi, A. Cabot, and R. Zambrini, Ann. Phys. (Berlin, Ger.) **531**, 1900307 (2019).
[77] A. Ricottone, M. S. Rudner, and W. A. Coish, Phys. Rev. A **102**, 012215 (2020).